Design and Finite Element Analysis of Qusi-Flat Permanent Magnet Linear Generator for Solar Thermal Energy Conversion

Wunna Swe
Department of Electrical Power Engineering, Mandalay Technological University, Myanmar

***Abstract*— Electricity is an important role for development of the country. On the other hand, it is crucial to develop clean renewable energy sources due to the pending exhaustion of fossil fuels and to their environmental impact. Due to easily accessible from everywhere on earth surface, solar energy is one of the most favorable renewable sources. Because of using photovoltaic for electricity is costly and thus such application is limited in practice, solar-thermal power generation is focused in this paper. The design and simulation of Quasi-flat Linear Permanent Magnet Generator driven by Stirling engine are supported to improve the existing solar-thermal electricity generation systems.**

In this paper, Quasi-flat Linear Permanent Magnet Generator is designed based on the expected output power and the solar irradiance characteristic at the placement site. The generator design is intended to generate maximum power for 24kW. Modeling of linear generator is described and simulation results of performance analyses are also tabulated by Finite Element Magnetic Method. The analysis of magnetic flux density and intensity were not approached to zero limit and lower values that are respectively 0.5T in stator core and 2e+005Amp/m in rotor core by using NdFeB magnet which its circulation of flux value is good condition than other magnets. According to the performance analysis, the design of generator is feasible and acceptable.

***Keywords*—Solar thermal energy, linear generator design, Finite Element Method, Free-piston Stirling engine, solar parabolic dish-Stirling**

I. INTRODUCTION

Because of the depletion of fossil energy resources and the global warming, searching alternative solutions to develop clean renewable energy resource becomes an important issue. The rapid development of renewable energies represents a challenge for the scientific community to develop new technology or improve the old ones. Among the many technologies, permanent magnet linear generators (PMLG) represent, of course, an important case of study. PMLGs convert mechanical energy into electrical energy. They find application in all the fields that involves linear motion, such as: cogeneration systems that use free- piston combustion engine (FPCE), wave energy converters and hybrid automotive field. The choice of a linear motion generator overcomes a possible mechanical linkage system (crankshaft), which is source of losses, noise and failures.

As grid electricity power system cannot be supplied all over the country, the need of rural electrification is high. In the middle regions of Myanmar, solar thermal potential is relatively high, if so we can use the solar thermal as an energy source. There are the varieties of ways to harvest energy from solar thermal. The stand-alone or off-grid concentrated solar power plants require to build for supplying the needed of electricity in rural.

II. DISH STIRLING SOLAR THERMAL SYSTEM

Solar energy is the most abundant renewable energy source which is readily available anywhere the sun shines. The yearly solar fluxes are estimated around 3.85×10^{24}J. Insolation in most countries is from 150 to 300W/m^2 that means from 1.3 to 2.5MWh/m^2/year [7]. In 2012, the word's human primary energy consumption was 539×10^{18}J [8], more than 7000 times less of the yearly word's solar energy.

There are different typologies of solar thermal generation systems, the main are: parabolic trough, linear Fresnel reflectors, solar tower and dish stirling system. The most promising system is dish Stirling (shown in Figure 1.), thanks its higher efficiency. The dish Stirling systems use a mirror array to reflect and concentrate solar insolation to a receiver, in order to achieve the temperature required efficiency convert heat to work.

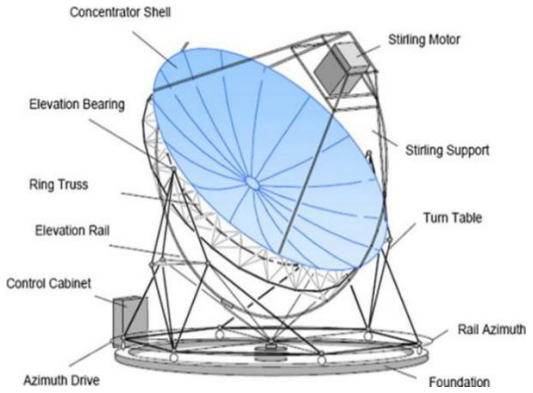

Figure 1. Solar Dish Stirling Generation System [10]

The ideal concentrator shape is a parabolic of revolution which concentrates sunlight on the focus of parabolic.

Concentration ratio is typically over 2000 and, hence, the concentrator must track the sun in two axes. At the focus is a receiver which is heated up to over 700 °C [10]. The solar-to-electric conversion efficiency of Dish Stirling systems can achieve 30% [11], which represent the highest value of all solar energy converters. The advantages of dish Stirling technology are [12]:

- Small land requirement (2.5 Ha/MW), due to high efficiency;
- Short construction times (10 months for a 20 MW plant);
- Low maintenance and operating costs;
- More stable output than photovoltaic systems.

III. PROPOSED SYSTEM

Among the different generation process, the proposed system driven by a free-piston Stirling engine is one of the most significant challenges in the research area. In such systems, the thermal energy, coming from primary energy source for example renewable energy, is converted into mechanical energy through a Stirling engine, and then a linear generator converts the mechanical energy into electrical energy, finally, the generator is connected to the electric grid or to the load by means of an electric converter.

The use of the linear generator, instead of the traditional systems of linear to alternating motion conversion (rod-crank system), allows achieving several advantages, including: improving the system reliability, noise and cost reduction. Finally, this kind of system, if well-designed, allows improving the system efficiency. The proposed system is shown in Figure 2.

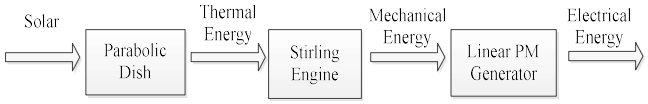

Figure 2. Energy Transformation Process of a Dish-Stirling Power Generation System

IV. DESIGN EQUATIONS OF LINEAR GENERATOR

In this section, the main concept about the design equations of quasi-flat linear electric generator and its main component of stator and rotor core and winding parameters for proposed system in details are described.

A. Primary Length and Width

To design primary length and width of quasi-flat linear electric generator, we need to calculate the design equations shown in table 1. In the table, Eph means Phase induced voltage, Iph means Phase current, N_c means number of turns per coil and τ_t means tooth pitch.

TABLE 1.DESIGN EQUATIONS FOR PRIMARY LENGTH AND WIDTH

No	Parameter	Equations
1	The apparent power	$S = mE_{ph}I_{ph}$
2	Maximum phase induced voltage	$E_{phm} = M_s W_s N_{ph} B_m v_{av}$
3	The rms phase induced voltage	$E_{ph} = \frac{M_s W_s N_{ph} B_m v_{av}}{\sqrt{2}}$
4	Current loading	$J = N_c I_{ph}/\tau_t$
5	The phase current	$I_{ph} = J\tau_t/N_c$
6	Number of turn per coil	$N_{ph} = N_c pq$
7	Number of turns per phase	$N_c = N_{ph}/qp$
8	The apparent power (substituted)	$S = \frac{M_s W_s \tau_t pqm B_m v_{av} J}{\sqrt{2}}$
9	The stator length	$L_s = \tau_t pqm$
10	The length of the stator	$L_s = \frac{S_{in}\sqrt{2}}{M_s W_s B_m J v_{av}}$

When the magnets are moving with speed v_{av} with respect to the phase coils the electromotive force is induced and its maximum value is shown in Figure 3 at maximum flux density Bm.

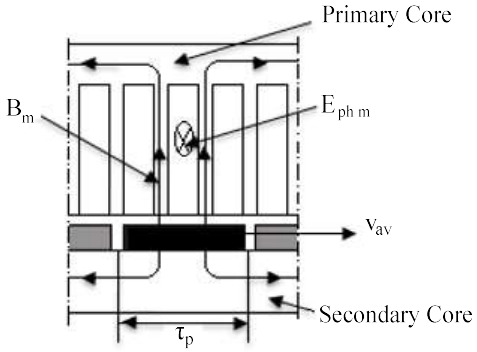

Figure 3. Generator Model

B. Pole Pitch and Tooth Pitch

The necessary equations for designing for pole pitch, pole pith, tooth pitch, number of stator slots and pole and tooth width are described in Table 2.

TABLE 2. DESIGN EQUATIONS FOR POLE PITCH AND TOOTH PITCH

No	Parameter	Equations
1	The pole pitch τp	$\tau_p = \frac{L_s}{p}$
2	The tooth pitch τt	$\tau_t = \frac{\tau_p}{mq}$

3	total number of stator slots	$S_T = 1\text{slot/pole/phase} \times 3\text{phase} \times 6\text{pole}$
4	Number of stator slot per phase	$\text{slot/phase} = 1\text{slot/pole/phase} \times 6\text{poles}$
5	Slot Width (b_s)	$b_s = \frac{2}{3}\tau_t$
6	Tooth Width (b_t)	$b_t = \frac{1}{3}\tau_t$

Slot width b_s and tooth width b_t can be calculated the value of tooth pitch τ_t as shown in Figure 4.

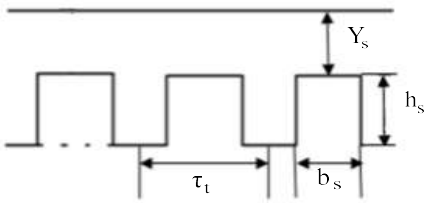

Figure 4. Picture Showing Primary Core Slots

C. Yoke Dimensions

The dimensions of yoke are depending on the total number of flux and flux density in primary and secondary elements. The thickness of the primary and secondary yoke can be determined by equations shown in Table 3.

TABLE 3. DESIGN EQUATION FOR PRIMARY AND SECONDARY YORK

No	Parameter	Equations
1	The flux in the air-gap	$\varphi_g = \tau_p W_s B_g$
2	The flux in the primary yoke	$\varphi_y^s = Y_s W_s B_y^s$
3	The stator yoke thickness Ys	$Y_s = \frac{B_g}{B_y^s}\frac{\tau_p}{2}$
4	The rotor yoke thickness Yr	$Y_r = \frac{B_g}{B_y^r}\frac{\tau_p}{2}$

The model for finding of primary York and secondary York is shown in Figure 5.

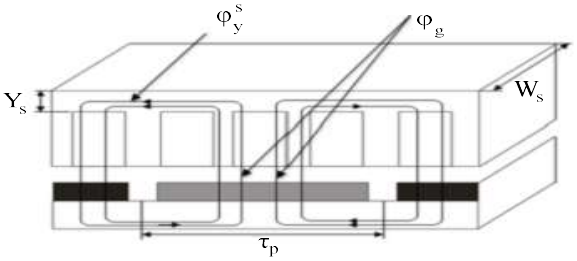

Figure 5. Model for Finding the Yoke Dimensions

D. Design equations for armature winding

To determine the armature winding, the equations shown in Table 4 are necessary for linear generator.

TABLE 4. DESIGN EQUATIONS FOR ARMATURE WINDING

No	Parameter	Equations
1	The number of turns per phase Nph	$N_{ph} = \frac{E_{ph}\sqrt{2}}{M_s W_s B_m v_{av}}$
2	Number of turns per coils Nc	$N_c = \frac{N_{ph}}{qp}$
3	The value of rms current I (Y connection)	$I = \frac{S}{3E_{ph}}$
4	The cross-section area of the wire Aw	$A_w = \pi r_w^2 = \frac{I}{J_W}$
5	Wire diameter	$d_w = 2\sqrt{\frac{I}{\pi J_w}}$
6	Current density J in a wire	$J = \frac{I}{A_w}$
7	The cross-section area of coil	$A_c = \frac{\pi\left(\frac{d_w}{2}\right)^2 N_c}{K_{cu}}$
8	Cross section area of the slot	As = winding width × winding height
9	The height of the slot hs	$h_s = \frac{A_s}{b_s}$

The relationship between cross sectional area of the slot, the slot width and the slot height are shown in Figure 6.

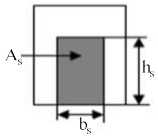

Figure 6. Slot Model

E. Permanent Magnet Dimensions

Carter's coefficient Kc has to be found in order to calculate the equivalent air-gap g_{eq}. To calculate the thickness, length and difference between two magnets can be calculated by equations shown in Table 5.

TABLE 5. DESIGN EQUATIONS OF PERMANENT MAGNET DIMENSIONS

No	Parameter	Equations
1	Carter's coefficient Kc	$K_c = \frac{\tau_t(5g + b_s)}{\left[\tau_t(5g + b_s) - b_s^2\right]}$
2	the equivalent air-gap g_{eq}	$g_{eq} = K_c g$
3	Magnet thickness	$h_m = \frac{g_{eq} B_r B_g}{\mu_0 \lvert H_c \rvert (B_r - B_m)}$

4	the magnetic air gap	$g_m = h_m + g$
5	The length of Permanent Magnet	$\tau_m = C_m \tau_p$
6	The distance between two magnets	Distance = $\tau_p - \tau_m$

V. DETERMING THE INITIAL PARAMETER OF LINEAR GENERATOR

Table 6 described the initial data of the generator to be designed. The design parameter is based on the requirement of dish-stirling solar thermal system.

TABLE 6. DESIRABLE PARAMETER OF LINEAR GENERATOR

Parameters	Symbol	Values
Apparent power	S	30 k VA
Induced phase voltage	Eph	230.94 V
Velocity amplitude	vrms	2.2 m/s
Average velocity	v_{av}	1.4 m/s
Number of phases	m	3
No of slots/ pole/ phase	q	1
No of magnetic poles	p	6
Avg flux density in ag	B_g	0.8 T
Coefficient for air-gap flux density	C_m	0.9
air-gap flux density under magnets	B_m	0.88 T
Air-gap	g	2 mm
Permissible flux density in stator core	B_{ys}	1.8 T
Permissible flux density in rotor core	B_{yr}	1.2 T
Current loading (stator)	J	120 kA/m
Wire current density	J_w	5 A/mm^2
Winding filling factor	K_{cu}	0.6
Number of armatures	M_s	4
Magnet Remanence (NdFeB)	B_r	1.251 T
Coercivity (NdFeB)	H_c	950kA/m
Magnetic recoil permeability	μ_R	1.08846

VI. DESIGN RESULTS OF LINEAR GENERATOR

During the design of a PM machine, there are many unknown parameters which play a role in the final desired design. In this case, there are even more parameters to consider because of the nature of the device being linear, modular and weight dependent. In the beginning of the design, while developing theoretical magnetic circuit geometries, design constraints were used to help determine the remaining parameters.

From the desirable parameters in Table 6, Quasi-flat Linear Permanent Magnet Generator designed by using design equations which are shown in Table 1 to Table 5. The results of design data are shown in Table 7.

TABLE 7. DESIGN DATA OF LINEAR GENERATOR

No	Parameters	Symbols	Values	Units
Stator Core:				
1	Length	L_s	360	mm
2	Width	W_s	200	mm
3	Stator yoke	Y_s	13	mm
4	Slot width	b_s	13	mm
5	Tooth width	b_t	7	mm
6	Tooth height	h_s	72.5	mm
7	Total number of stator slots	S_T	18	slots
8	Cross-section area of slot	A_s	942.5	mm
9	Permissible flux stator yoke	B_y^s	1.8	T
10	Laminated Steel core	US steel type 2-S	-	-
11	Pole pitch	τ_p	60	mm
12	Tooth pitch	τ_t	20	mm
Rotor Core:				
13	Rotor yoke	Y_r	20	mm
14	Permissible flux rotor yoke	B_y^r	1.2	T
15	Magnet length	τ_m	54	mm
Winding:				
16	Turn number/coil	N_c	57	turns
17	Turn number/phase	N_{ph}	342	turns
18	Y connected rms current	I	43.3	A
19	Resistance of winding per phase	R_{ph}	0.76	Ω/ph
20	Air-gap flux	φ_g	9.6	mWb
21	Primary flux	φ_y^s	4.68	mWb
22	Secondary flux	φ_y^r	4.8	mWb
23	Leakage reactance	X_L	0.9875	Ω
24	Inductance	L	23.93	mH
25	8AWG diameter	d_w	3.3	mm
Permanent Magnet:				
26	Magnet thickness	h_m	7	mm
27	Carter's coefficient	K_c	1.58	-
28	Distance between PM	-	6	mm

VII. FINITE ELEMENT ANALYSIS WITH VARIOUS PERMANENT MAGNET

In previous section, quasi-flat linear permanent magnet generator is designed with theoretical sizing equations. After slotting, designs are calculated with the sizing equations, their same design will be evaluated by using FEMM software in this section. In this analysis, the performances of 30 kVA LPMG with slotted stator are analyzed with FEMM.

The quasi-flat LMPG could be classified based on the shape of its stator core and consists of four-sided flat although modelling only one-sided flat of the generator are analysised. It has also axial symmetry, therefore allowing for a two-dimentational finite-element analysis to be created. Thus, the surface mounted permanent magnets (NdFeB) attached to the translator, one of the air-gap clearances and half of the stator needed to be modelled.

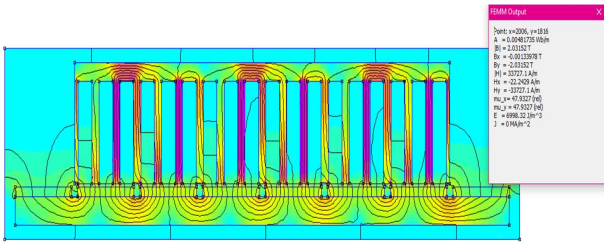

Figure 6. Flux Density Distribution in Primary Core

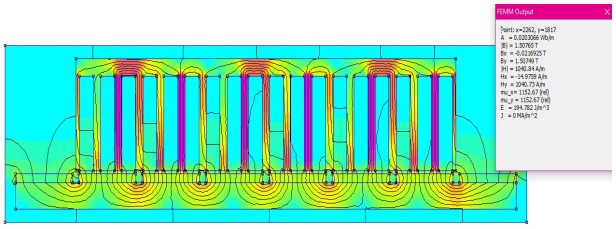

Figure 7.Flux Density Distribution in Secondary Core

Figure 6 and 7 shows the flux density distribution of primary and secondary core. The maximum flux density in the primary core is 2 T and in the secondary core is1.5 T. The flux density values in the secondary and the primary parts are too high with respect to the assumed permissible values. The flux density of the generator in the primary core especially a gap between the two sloths on account of passing the permanent magnet is higher than the value of flux density in secondary core.

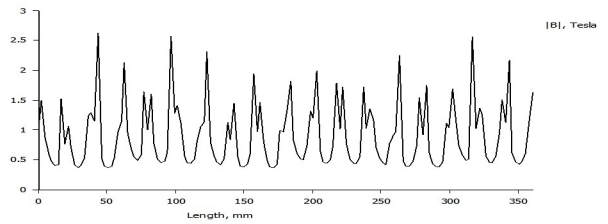

Figure 8. Magnetic Flux Density in Stator with NdFeB Magnet

Figure 8 shows the magnetic flux density of quasi-flat LPMG and also illustrates the magnitude of magnetic flux density plot for whole length of stator part . The highest value of magnetic flux density is 2.5T and its value is also unstable between the magnets. However, flux densities do not approach to 0T and their values are not lower than the 0.5T. The average value of flux densities is 1.5T in the middle of the magnet.

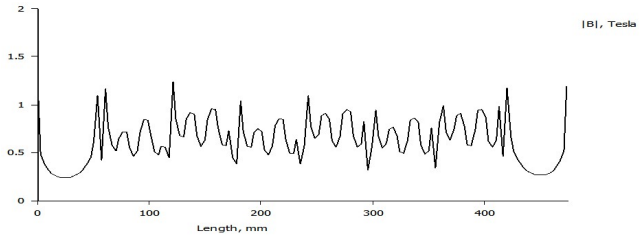

Figure 9. Magnetic Flux Density in Rotor by NdFeB Magnet

Figure 9 shows the magnetic flux density of quasi-flat LPMG and also illustrates the magnitude of magnetic flux density plot for whole length of rotor core by using FEMM software. The highest value of magnetic flux density is 1.3T and its value is also unstable between the magnets. However, flux density does not approach to zero and lower than the 0.25T.The average value of flux densities is 1T in the middle of the magnet.

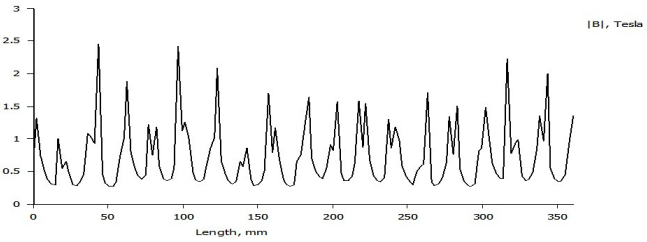

Figure 10. Analysis of Magnetic Flux Density in Stator by SmCo Magnet

Figure 10 shows the magnetic flux density of quasi-flat LPMG and also illustrates the magnitude of magnetic flux density plot in stator core by using FEMM software. The highest value of magnetic flux density is almost 2.5T and others flux density values are also unstable between the magnets. However, flux density does not approach to zero but its lowest value is 0.25T. The average value of magnetic field intensities is about 1.5T. This value is lower than the value of NdFeB magnet.

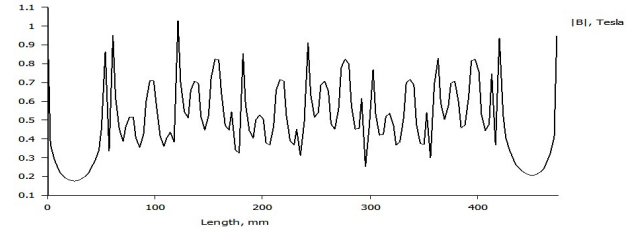

Figure 11. Analysis of Magnetic Flux Density in Rotor by SmCo Magnet

Figure 11 shows the analysis result of magnetic flux density of quasi-flat LPMG and also illustrates the magnitude of magnetic flux density plot in rotor core by using FEMM software. The highest value of magnetic flux density is over 1T and other flux density values are also unstable between the magnets. However, flux density does not approach to 0T but its lowest value is 0.2T and the average value of flux densities is 0.8T. This value is lower than the value of NdFeB magnet.

According to the results from the FEMM analysis, using NdFeB magnet for quasi-flat LPMG shows better performance than using SmCo magnet. Therefore, the NdFeB magnet is used in the quasi-flat linear permanent magnet generator for solar-powered Stirling engine.

VIII. CONCLUSIONS

In this paper a solar thermal generation system, consisting of a Stirling engine and a tubular permanent magnet linear generator (TPMLG) was investigated. The performance of Tubular linear PM 3 phase generator driven by solar thermal energy has been studied. The linear generator with linear machine structure was designed using the magnetic circuit by applying FEMM.

The flux density value in the secondary and the primary parts is too high with respect to the assumed permissible value Although changing the type of the magnet, the highest values of magnetic flux density and magnetic field intensity are occurred by run analysis result of NdFeB magnets. Therefore, the NdFeB magnet is used the linear tubular permanent magnet generator for solar-powered Stirling engine.

REFERENCES

[1]. UBS - Wealth Management Research. Solar thermal - a new power giant is awakening. Zurich: UBS, 2009.
[2]. W. Cawthorne, P. Famouri, and N. Clark, 2001, “Integrated design of linear alternator/engine system for HEV auxiliary unit”.
[3]. Renewable energy." http://en.wikipedia.org/ wiki/ Renewable_energy (accessed Oct 14, 2011).
[4]. A. D. Minassians, "Stirling Engines for Low-Temperature Solar-ThermalElectric Power Generation", Pd.D. Thesis, Electrical Engineering and Computer Sciences, University of California at Berkeley, 2007.
[5]. Arvizu, D. , et al. Technical Summary. In IPCC Special Report on Renewable Energy Sources and Climate Change Mitigation. Cambridge, United Kingdom and New York, NY, USA: Cambridge University Press, 2011.
[6]. UBS - Wealth Management Research 2009
[7]. Key World Energy Statistics
[8]. International Energy Statistics, www.eia.gov.
[9]. A. D. Minassians, "Stirling Engines for Low-Temperature Solar-ThermalElectric Power Generation", Pd.D. Thesis, Electrical Engineering and Computer Sciences, University of California at Berkeley, 2007.
[10]. W. Beale, G. Chen, "Small Stirling Free-Piston Engines for Cogeneratio", Sunpower Inc., Athens (Ohio), June 1992.
[11]. S. A. Zulkifli, M. N. Karsiti and A. R. A. Aziz, "Starting of a Free-Piston Linear Engine-Generator by Mechanical Resonance and Rectangular Current Commutation", IEEE Vehicle Power and Propulsion Conference (VPPC), September 3-5, 2008, Harbin, China.
[12]. J. Wang, D. Howe, "A linear permanent magnet generator for a free-piston energy converter", Conference on Electric Machines and Drives, 2005 IEEE International, 15-15 May 2005, San Antonio, TX.
[13]. G. Walker, Stirling Engines. Oxford University Press, 1980.
[14]. Pirisi, A., G. Gruosso, and R.E. Zich, Novel modeling design of three phase tubular permanent magnet linear generator for marine applications, in Power Engineering, Energy and Electrical Drives, 2009. POWERENG '09. International Conference onMarch 2009. p. 78-83.
[15]. Rajkumar Parthasarathy, Louisiana State University and Agricultural and Mechanical College: “ Linear PM generator for wave energy conversion”, May. 2012, pp. 14-28.
[16]. Boldea, lon, Syed A. Nasar, Linear Electric Actuators and Genera/ors, Cambridge: Cambridge University Prss, 1997, pp.33-36.